Evaluating the Role of Nanomontmorillonite in Bulk in Situ Radical Polymerization Kinetics of Butyl Methacrylate through a Simulation Model

ARTICLE *in* INDUSTRIAL & ENGINEERING CHEMISTRY RESEARCH · JULY 2014

Impact Factor: 2.59 · DOI: 10.1021/ie501360j

4 AUTHORS:

Mohammad Nahid Siddiqui
King Fahd University of Petroleum and Minerals
85 PUBLICATIONS **855** CITATIONS
SEE PROFILE

Halim Redhwi
King Fahd University of Petroleum and Minerals
62 PUBLICATIONS **510** CITATIONS
SEE PROFILE

George D. Verros
Aristotle University of Thessaloniki
48 PUBLICATIONS **298** CITATIONS
SEE PROFILE

Dimitris S. Achilias
Aristotle University of Thessaloniki
141 PUBLICATIONS **2,948** CITATIONS
SEE PROFILE

I&EC research
Industrial & Engineering Chemistry Research

Article

pubs.acs.org/IECR

Evaluating the Role of Nanomontmorillonite in Bulk in Situ Radical Polymerization Kinetics of Butyl Methacrylate through a Simulation Model

Mohammad Nahid Siddiqui,[†] Halim Hamid Redhwi,[‡] George D. Verros,[§] and Dimitris S. Achilias*[,§]

[†]Chemistry Department, Center of Excellence in Nanotechnology (CENT) and [‡]Chemical Engineering Department, King Fahd University of Petroleum and Minerals, Dhahran 31261, Saudi Arabia

[§]Laboratory of Organic Chemical Technology, Department of Chemistry, Aristotle University of Thessaloniki, 541 24 Thessaloniki, Greece

ABSTRACT: The effect of adding a nanoclay on the radical polymerization kinetics above the polymer's glass transition temperature was investigated through a simulation model. As an example, the polymerization of butyl methacrylate in the presence of organomodified nanomontmorillonite was studied. The mathematical model developed was based on the elementary chemical reactions taking place and appropriate species mass balance equations. To account for the effect of diffusion-controlled phenomena, appropriate theoretical equations were derived based on sound principles. The number of fitting parameters was kept to a minimum of four. It was found that the addition of the nanoclay mainly affects the initiator efficiency and the reaction−diffusion term of the termination rate constant. Model predictions for monomer conversion were found to be in very good agreement with published experimental data. Moreover, the effect of the nanoclay on the evolution of the polymer average molecular weights during the reaction was discussed in detail.

1. INTRODUCTION

Synthesis and characterization of nanocomposite materials based on a polymer matrix have attracted the attention of many researchers because of their unique behavior. The addition of only a small amount of nanoclay (usually less than 5 wt %) to a polymer matrix has a significant impact on the mechanical, thermal, fire resistance, and barrier properties of the polymer.[1,2] Among other techniques used to prepare polymer/clay nanocomposites, the in situ polymerization method is one of the most desirable because final product requirements can be easily met. By in situ polymerization, the clay is swollen in the monomer for a certain time depending on the polarity of the monomer molecules and the surface treatment of the clay. The monomer migrates into the galleries of the layered silicate so that the polymerization reaction occurs between the intercalated sheets. Long-chain polymers within the clay galleries are thus produced.[3−6]

Although the effect of the nanofiller and specifically of the nanoclay on the nanocomposite material properties has been extensively studied, only a few works have appeared on its polymerization kinetics. In recent research from our group, several monomers, including methyl methacrylate (MMA), ethyl methacrylate (EMA), and butyl methacrylate (BMA), have been studied.[7,8] Moreover, the copolymerization kinetics of styrene with either EMA or BMA has also been investigated.[9,10] Depending on the monomer type and nanoclay type and amount, it was found that the reaction kinetics could be slightly retarded or accelerated. Moreover, higher amounts of nanomontmorillonite usually results in lower ultimate conversion values.

Radical polymerization kinetics has been the subject of extensive studies for a long time.[11−16] Besides the chemical reaction mechanism, diffusion-controlled phenomena on all elementary steps usually play an important role in the reaction rate and final product properties. Moreover, from the methacrylates family, mainly methyl methacrylate has been extensively studied. Very recently, Simon et al.[17−19] have extended previous simulation models developed to predict the radical polymerization kinetics of MMA[14] to account for the reaction taking place in nanoporous confinements. Either hydrophilic or hydrophobic pores were investigated. Diffusional limitations in all elementary reactions, i.e., initiation, propagation, and termination associated with the cage, glass, and gel effect, were considered. The Doolittle free-volume equation was used for the estimation of the diffusion coefficients. Their model described experimental data taken from differential scanning calorimetry (DSC) measurements at different pore diameters very well.

The picture is quite similar, though inherently different, in the in situ polymerization technique for producing polymer/clay nanocomposites. Polymerization takes place between the intercalated clay sheets with the initiator molecules thermally decomposing to form primary radicals that eventually react with monomer molecules that have migrated into the galleries of the layered silicate. Thus, either exfoliated or intercalated structures are formed with macromolecules formed within the clay galleries. However, there always remain some questions about whether clay acts as a radical scavenger, decreasing the population of effective primary radicals and eventually initiator efficiency, or if it poses extra hindrance in the movement of either long-chain or small molecules in order to react.

Received: April 1, 2014
Revised: June 17, 2014
Accepted: June 20, 2014
Published: June 20, 2014

dx.doi.org/10.1021/ie501360j | *Ind. Eng. Chem. Res.* 2014, 53, 11303−11311

Although a number of experimental works have been published on the formation of polymer-based nanocomposites with different types and amount of nanofiller, theoretical simulation works of radical polymerization kinetics in the presence of nanoclay are rare. Therefore, the objective of this investigation is to develop a model to account for the effect of the nanofiller, specifically nano-MMT, on the radical polymerization kinetics of butyl methacrylate. A set of differential equations was set to account for the time variation of the species present in a batch polymerization reactor based on the elementary reactions taking place during the reaction. The effect of diffusion-controlled phenomena on the termination, propagation, and initiation reaction were considered based on theoretical equations and the diffusion coefficients of the reacting species.[13] The effect of the presence of the nanoclay on the polymerization kinetics was evaluated in a comparison to the theoretical simulation results and experimental data obtained from a previous publication from our group.[8]

2. POLYMERIZATION MODEL

The first step in constructing a mathematical model describing radical polymerization kinetics is identifying the kinetic mechanism. A typical kinetic mechanism of free-radical homopolymerization is illustrated in Table 1. The major elementary reactions of chain initiation, propagation, chain transfer to monomer, and termination either by combination or disproportionation are included. All symbols used are explained in Nomenclature. The second step is to develop the species mass balance equations from the kinetic scheme. On the basis of the mechanism illustrated in Table 1, the equations describing the conservation of species in a batch reactor can be derived (Table 2). As is noted in this table, the quasi-steady-state approximation (QSSA) is applied to primary radicals only. The QSSA is not extended to calculation of the macroradical population, as the approximation is not accurate at high monomer conversions. Thus, all equations describing the variation of the radical concentration with time remain in differential form.

Table 1. Typical Kinetic Mechanism of Free-Radical Polymerization[a]

Initiation

$$I \xrightarrow{k_d} 2PR^\bullet$$

$$PR^\bullet + M \xrightarrow{k_I} P_1^\bullet$$

Propagation

$$P_n^\bullet + M \xrightarrow{k_p} P_{n+1}^\bullet$$

Chain transfer to monomer

$$P_n^\bullet + M \xrightarrow{k_{fM}} D_n + M^\bullet$$

$$M^\bullet + M \xrightarrow{k_{pM}} P_1^\bullet$$

Termination by combination or disproportionation

$$P_n^\bullet + P_m^\bullet \begin{cases} \xrightarrow{k_{tc}} D_{n+m} \\ \xrightarrow{k_{td}} D_n + D_m \end{cases}$$

[a] I denotes initiator, M monomer, and $PR^\bullet$ primary radicals; $P_n^\bullet$ and D_n denote live radicals and polymer chains of length n, respectively; k_d, k_I, k_p, k_{fM}, k_{tc}, and k_{td} are the rate constants for the initiator decomposition, chain initiation reaction, propagation, chain transfer to monomer, termination by combination, and termination by disproportionation, respectively.

Table 2. Species Mass Balance Equations in an Isothermal Batch Reactor[a]

Initiator

$$\frac{1}{V}\frac{d(VI)}{dt} = -k_d I$$

Monomer−fractional monomer conversion (X)

$$\frac{1}{V}\frac{d(VM)}{dt} = -(k_p + k_{fM})MP_0$$

Macromolecular species balance

$$\frac{1}{V}\frac{d(VPR^\bullet)}{dt} = 2fk_d I - k_I PR^\bullet M = 0$$

$$\frac{1}{V}\frac{d(VP_n)}{dt} = (k_I PR^\bullet M)\delta(n-1) + k_p M(P_{n-1} - P_n) - (k_{tm}M + k_t P_0)P_n$$

$$\frac{1}{V}\frac{d(VD_n)}{dt} = k_{fM}MP_n + \frac{1}{2}k_{tc}\sum_{r=1}^{n-1} P_r P_{n-r} + k_{td}P_0 P_n$$

[a] P_0 is the total concentration of "live" polymer: $P_0 = \sum_{r=0}^{\infty} P_r$ and $\delta(n)$ is the Kronecker delta

The next step is to recast the infinite number of macomolecular chain population balance equations into a finite set of modeling equations. This could be achieved by using the well-known method of moments of the chain length distribution (CLD) or molecular weight distribution (MWD). Moments of the CLD of the "live" radicals or "dead" polymer macromolecules are defined as[12,14]

$$\lambda_k = \sum_{n=0}^{\infty} n^k P_n; \quad \mu_k = \sum_{n=0}^{\infty} n^k D_n; \quad k = 0, 1, 2 \tag{1}$$

On the basis of the species balance equations and the method of moments, one could derive the following set of differential equations for an isothermal batch reactor:[12,14]

Initiator

$$\frac{d(I)}{dt} = -k_d I - \frac{I}{V}\frac{dV}{dt} \tag{2}$$

Fractional monomer conversion (X)

$$\frac{d(X)}{dt} = (k_p + k_{fM})(1 - X)\lambda_0 \tag{3}$$

Live radical moment equations

$$\frac{d(\lambda_0)}{dt} = r_{\lambda_0} = 2fk_d I - k_t\lambda_0\lambda_0 - \frac{\lambda_0}{V}\frac{dV}{dt} \tag{4}$$

$$\frac{d(\lambda_1)}{dt} = r_{\lambda_1} = 2fk_d I + k_p M\lambda_0 + k_{fM}M(\lambda_0 - \lambda_1) - k_t\lambda_0\lambda_1 - \frac{\lambda_1}{V}\frac{dV}{dt} \tag{5}$$

$$\frac{d(\lambda_2)}{dt} = r_{\lambda_2} = 2fk_d I + k_p M(2\lambda_1 + \lambda_0) + k_{fM}M(\lambda_0 - \lambda_2) - k_t\lambda_0\lambda_2 - \frac{\lambda_2}{V}\frac{dV}{dt} \tag{6}$$

Polymer moment equations:

dx.doi.org/10.1021/ie501360j | Ind. Eng. Chem. Res. 2014, 53, 11303−11311

$$\frac{d(\mu_0)}{dt} = r_{\mu_0} = k_{fM}M\lambda_0 + \left(k_{td} + \frac{1}{2}k_{tc}\right)\lambda_0^2 - \frac{\mu_0}{V}\frac{dV}{dt} \quad (7)$$

$$\frac{d(\mu_1)}{dt} = r_{\mu_1} = k_{fM}M\lambda_1 + k_t\lambda_0\lambda_1 - \frac{\mu_1}{V}\frac{dV}{dt} \quad (8)$$

$$\frac{d(\mu_2)}{dt} = r_{\mu_2} = k_{fM}M\lambda_2 + k_{tc}\lambda_1^2 + k_t\lambda_0\lambda_2 - \frac{\mu_2}{V}\frac{dV}{dt} \quad (9)$$

From the above set of equations the variation with time of the initiator concentration, monomer conversion, and averages of the MWD can be obtained. The number and the weight-average degree of polymerization ($\bar{X}_n$,$\bar{X}_w$) as well as the polydispersity, D, of the MWD are given as follows:

$$\bar{X}_n = \frac{\mu_1 + \lambda_1}{\mu_0 + \lambda_0}; \quad \bar{X}_w = \frac{\mu_2 + \lambda_2}{\mu_1 + \lambda_1}; \quad D = \frac{\bar{X}_w}{\bar{X}_n} \quad (10)$$

Number and weight-average molecular weight of the final polymer are simply calculated by multiplying the number or weight-average chain length by the monomer molecular weight.

Finally, because volume contraction is generally significant during bulk polymerization, the variation of the reaction volume with conversion is given by

$$V = V_0(1 - \varepsilon X) \quad (11)$$

where ε is the volume contraction factor given as a function of the monomer, ρ_m, and polymer, ρ_p, density as

$$\varepsilon = \frac{\rho_p - \rho_m}{\rho_p} \quad (12)$$

Then

$$\frac{dV}{dt} = -V_0\left[\varepsilon\frac{dX}{dt} + X\frac{d\varepsilon}{dt}\right] = -V_0\varepsilon\frac{dX}{dt}$$

and

$$\frac{1}{V}\frac{dV}{dt} = \frac{-\varepsilon(dX/dt)}{1 - \varepsilon X} \quad (13)$$

The system of eight coupled ordinary differential equations (eqs 2−9) are numerically integrated to give the time dependence of all reacting species using standard numerical techniques. To calculate the complete molecular weight distribution, the instantaneous property method (IPM) was applied. A complete description of this method is given in full detail elsewhere.[20−22] The variation of the kinetic rate constants as a function of the process conditions is considered according to the model described in the next section.

2.1. Diffusion-Controlled Reactions. Kinetic rate constants usually depend only on temperature through an Arrhenius-type expression. However, in radical polymerization reactions occurring in bulk, diffusion-controlled phenomena play an important role during the whole conversion range. Thus, parameters f, k_p, and k_t are considered to be diffusion-controlled associated with the cage, glass, and gel effect, respectively. Several theories and models have been proposed in the literature to quantify the effect of diffusion on the mobility of reacting species in a polymerizing system.[13] Detailed models usually require a large number of often adjustable parameters. The theoretical equations derived in Achilias and Sideridou[23] were used in this work, which is based on theoretically sound equations, although they do not need a large number of parameters because the experimental data which are going to be simulated are rather limited. Accordingly, the final expressions for the termination and the propagation rate constants are written as

$$\frac{1}{k_{te}} = \frac{1}{k_{t0}} + \frac{1}{4\pi N_A r_t \bar{D}_p} \quad (14)$$

$$\frac{1}{k_p} = \frac{1}{k_{p0}} + \frac{1}{4\pi N_A r_m D_M} \quad (15)$$

where k_{t0} and k_{p0} are the intrinsic kinetic rate constants for termination and propagation, respectively; r_t and r_p represent the effective reaction radii for termination and propagation; and finally, $\bar{D}_p$ and D_M denote the "live" radicals and monomer self-diffusion coefficients in the presence of a nanoadditive, respectively.

It should be noted here that work considering the diffusion-controlled reactions in nanopores has appeared in the open literature.[17,18] The challenge in modeling the role of nano-montmorillonite in situ bulk free-radical polymerization kinetics is not only to describe the effect of nanomontmorillonite on reaction kinetics but also to model the diffusion-controlled reactions in the presence of this additive.

The "live" radicals self-diffusion coefficient ($\bar{D}_p$) was calculated by combining the entropic barrier model of Gam et al.[24] with the free-volume theory.[25−28] More specifically, Gam et al.[24] showed that for an activated process due to nanoadditive presence, the following equation holds:

$$\bar{D}_p = \bar{D}_{p0}\exp(-\Delta F/RT) \quad (16)$$

where $\bar{D}_{p0}$ represents self-diffusion in the absence of barriers (without nanoadditive). Because macroradicals chain motion during the nanocomposite in situ formation occurs between cavities of size Ca, separated by bottlenecks of size Ba, the diffusion coefficient decreases exponentially with ΔF (= $F_2 - F_1$), where F_1 and F_2 are the confinement free energy for a chain in a cavity and bottleneck, respectively. According to scaling arguments, F_1 and F_2 are proportional to $N\mathrm{Ca}^{-1/\nu}$ and $N\mathrm{Ba}^{-1/\nu}$, where N is the degree of polymerization and ν is 0.5 for a Gaussian chain.[29−31] The scaling form for D_p/D_{p0} at low nanoadditive volume fraction is given as[24,29−31]

$$\ln\left(\frac{\bar{D}_p}{\bar{D}_{p0}}\right) = s - A_{nc}N; \quad s = -\alpha\varphi_p^{1/3} \quad (17)$$

where α and A_{nc} are adjustable parameters.

Following Gam et al.,[24] the effect of nanoadditive on macroradicals self-diffusion coefficient was assumed to vary as

$$\bar{D}_p = \bar{D}_{p0}e^{-\alpha\varphi_c^{1/3}} \quad (18)$$

where $\bar{D}_{p0}$ is the corresponding macroradicals self-diffusion coefficient at the same concentration and temperature but without nanoadditive and φ_c is the nanoadditive volume fraction. To keep the number of adjustable parameters to a minimum value, parameter α (eq 18) was set equal to zero as the nanoadditive concentration is relatively small. Moreover, the Doolittle free-volume equations were used for the estimation of the self-diffusion coefficients, $\bar{D}_{p0}$ and D_{M0}.[23]

$$\frac{1}{k_{te}} = \frac{1}{k_{t0}} + \frac{1}{4\pi N_A r_t \bar{D}_{p0}} = \frac{1}{k_{t0}} + \frac{\bar{M}^2}{D_{p00}\exp(-b/V_f)} \quad (19)$$

dx.doi.org/10.1021/ie501360j | Ind. Eng. Chem. Res. 2014, 53, 11303−11311

$$\frac{1}{k_p} = \frac{1}{k_{p0}} + \frac{1}{4\pi N_A r_m D_{M0}} = \frac{1}{k_{p0}} + \frac{1}{D_{M00}\exp(-b/V_f)} \quad (20)$$

Here, the Doolittle parameter, b, was set equal to b_0X with b_0 equal to 1, according to the literature.[17,18] The value of b thus increases with increasing conversion and is equal to 1 at complete conversion. For the dependence of the polymer diffusion coefficient, $\bar{D}_{p0}$, on the average molecular weight, $\bar{M}$, several exponents have been proposed. Here, we kept the value of 2 according to the concepts of the reptation theory.[23] Moreover, for the physical quantity representing $\bar{M}$, we used the number-average degree of polymerization of the live radicals defined in terms of the moments of the chain length distribution of free radicals as $\bar{M} = \lambda_1/\lambda_0$. All other constants were lumped into an overall adjustable parameter, i.e., D_{p00} and D_{M00} for the termination and the propagation rate constant, respectively.

Taking into account the effect of diffusion-controlled phenomena on the initiation reaction, a mathematical model had already been developed.[12,23] Following this model, the final expression for the initiator efficiency is expressed as

$$\frac{1}{f} = \frac{1}{f_0} + \frac{C}{D_I} = \frac{1}{f_0} + \frac{C}{D_{I0}\exp(-b/V_f)} \quad (21)$$

where f_0 is used to denote the initial initiator efficiency factor, D_I the self-diffusion coefficient of primary radicals, and C a lumped constant including geometrical features of the cage in which the primary initiator radicals are trapped and the initial initiation reaction rate constant.

In eq 21, the effect of possible loss of primary radicals through the recombination reactions is considered in f_0. When D_I is very large (i.e., at initial monomer conversions), then f is equal to f_0; however, when the mobility of the primary radicals is hindered as the polymerization proceeds, the diffusion coefficient (D_I) is decreased, leading to decreased initiation efficiency. For the diffusion coefficient, again the Doolittle theory was used with the pre-exponential factor divided by C left as an adjustable parameter.

The glass transition temperature of PBMA is around 30 °C,[8] and all polymerizations were carried out at 80 °C. Thus, all reactions took place at a temperature higher than the polymer glass transition temperature. Then, the free-volume fraction, V_f, is related to the temperature departure from the glass transition temperature, T_g, using the universal formula[17,18]

$$V_f = 0.025 + 0.00048(T - T_g) \quad (22)$$

The glass transition temperature of the reacting mixture increases during polymerization and can be related to conversion using the Fox equation assuming that the polymer/monomer mixture forms a homogeneous solution.

$$\frac{1}{T_g} = \frac{1}{T_{gm}} + X\left(\frac{1}{T_{gp}} - \frac{1}{T_{gm}}\right) \quad (23)$$

where T_{gm} and T_{gp} are the glass transition temperatures of the monomer and polymer, respectively, set equal to 150 K[18] and 303 K.[8]

Finally, the termination rate constant, k_t, is taken as the sum of the diffusion-controlled termination rate constant, k_{te}, and a so-called reaction−diffusion-controlled term, $k_{t,reac}$, following corresponding work in the literature.[13]

$$k_t = k_{te} + k_{t,reac} \quad (24)$$

The reaction−diffusion-controlled term, $k_{t,reac}$, also known as residual termination, accounts for the implicit movement of the macroradicals in space through the propagation reaction even when these macroradicals are "frozen" and cannot move through the center-of-mass diffusion.

$$k_{t,react} = Ak_pM \quad (25)$$

where A is a constant

It should be noted here that very interesting works on kinetic modeling, accounting also for the effect of diffusion-controlled phenomena, on controlled living/radical polymerizations such as atom-transfer radical polymerization (ATRP) or reversible addition−fragmentation chain transfer (RAFT) have been reported recently in the literature.[32−36]

3. METHODOLOGY

To build a successful simulation model, initially one has to identify a set of reliable parameters for the kinetic rate constants. The bulk homopolymerization of *n*-butyl methacrylate has been studied by several investigators, and kinetic parameters have been proposed in the literature.[37−44] Following these investigators, we assume that the polymerization mixture (initiator−monomer−polymer) forms a homogeneous solution.[37−44]

Therefore, in order to check the experimental data, we initially estimated the overall effective rate constant k_{eff} using eq 3 and the steady-state approximation for the total radical population, which has been proven to hold at low conversion values. Then eq 3 becomes

$$\frac{dX}{dt} = (k_p + k_{fM})(1 - X)\left(\frac{2fk_dI}{k_t}\right)^{1/2} \quad (26)$$

Assuming that the initiator concentration remains constant at small reaction times, eq 26 can be integrated to give

$$-\ln(1 - X) = k_{eff}t \quad (27)$$

with

$$k_{eff} = (k_p + k_{fM})\left(\frac{2fk_d}{k_t}I_0\right)^{1/2} \cong k_p\left(\frac{2fk_d}{k_t}I_0\right)^{1/2} \quad (28)$$

By plotting the left-hand side of eq 27, $-\ln(1 - X)$, versus time at low conversions, straight lines should appear having a slope equal to the effective rate constant. Such results appear in Figure 1 for the bulk polymerization of BMA and its nanocomposites with different relative amounts of the nanofiller. Experimental data in the range of 1−20% conversion were used and taken from ref 8. From the slope of these lines, the following values of the parameter k_{eff} were obtained: 0.0142 ± 0.0007, 0.0126 ± 0.0004, 0.0122 ± 0.0004, and 0.0129 ± 0.0003 min^{-1} for neat PBMA and PBMA with 1%, 3%, and 5% Cl15A, respectively. The corresponding correlation coefficients, R^2, were 0.9988, 0.9980, 0.9978, and 0.9984. It was observed that the effective rate constant for the neat polymer was slightly higher than that for the corresponding nanocomposites, whereas for the latter the values did not significantly change with the amount of the nanofiller. Using these values, an estimation of the kinetic rate constants at the initial stages of the polymerization can be obtained.

dx.doi.org/10.1021/ie501360j | Ind. Eng. Chem. Res. 2014, 53, 11303−11311

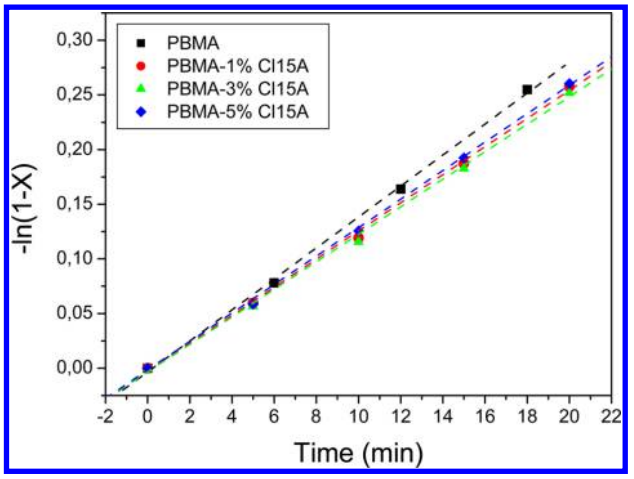

Figure 1. Estimation of the effective rate constant for the bulk polymerization of BMA and its nanocomposites with different amounts of Cl15A at 80 °C and 0.03 M initial BPO concentration. Experimental data from ref 8.

Then we looked for a reliable value for the initiator (BPO) decomposition rate constant, k_d. A number of different literature sources were considered, including polymer textbooks, papers, as well as data coming from BPO supply companies.[45−48] Most literature sources proposed a value near 2.1×10^{-5} s^{-1} at 80 °C, which is determined at low viscosity solutions such as benzene. The value selected here was taken from a very interesting and comprehensive work carried out some years ago by Stickler et al.[48] These authors carried out careful experiments using BPO in MMA polymerization at different temperatures, and they found that k_d depends not only on temperature but also on the reaction medium. The final temperature dependence they proposed was

$$\ln[k_d\ (s^{-1})] = 39.90 \pm 0.38 - \frac{18330 \pm 140}{T\ (K)} \quad (29)$$

which provides a value of $k_d = 6.14 \times 10^{-6}$ s^{-1} at 80 °C. It is obvious that this decomposition rate constant is substantially lower than the well-used value reported earlier, though this is a correct value estimated in a high-viscosity medium such as the one considered here. Moreover, according to Stickler and Dumont,[48] the initial initiator efficiency should be set equal to 1 (i.e., $f_0 = 1$). This value is expected to be significantly lower at high monomer conversions.

If we use these values and set the initial initiator concentration at 0.03 mol L^{-1},[9] then the value that can be estimated for the parameter $k_p/(k_t)^{1/2}$ for PBMA is 0.39 $L^{1/2}$ $mol^{-1/2}$ $s^{-1/2}$. BMA is a monomer extensively studied in literature as far as its polymerization kinetics.[37−43,49] The IUPAC benchmark data set for the propagation rate constant of BMA radical polymerization is[38]

$$k_p = 10^{6.58} \exp(-22.9\ kJ\ mol^{-1}/RT)\ L\ mol^{-1}\ s^{-1} \quad (30)$$

From this equation, the value at 80 °C is calculated as $k_p = 1558$ L mol^{-1} s^{-1}. Then, the estimated initial value of the termination rate constant, i.e., k_{t0}, is around 1.51×10^7 L mol^{-1} s^{-1}. This is in the same order of magnitude, close enough to the value of 2.98×10^7 L mol^{-1} s^{-1} estimated using the equation provided by Hutchinson et al.,[41,42] i.e., $k_{t0} = 1 \times 10^9 \exp(-1241/T)$ L mol^{-1} s^{-1}. However, in a detailed study on the chain-length dependent termination in butyl methacrylate bulk polymerization via single pulse−pulsed laser polymerization−electron spin resonance (SP-PLP-ESR), Barth et al.[40] proposed a value of k_t taking into account an exponential dependence on the polymer chain length, i. Accordingly, at 80 °C, if we assume a mean polymer chain length around $i = 3500$ (which is in the order of magnitude of this investigation) and the exponents $\alpha_s = 0.65$ and $\alpha_l = 0.20$ presented by these authors,[40] the value that could be estimated for k_{t0} is 9×10^6 L mol^{-1} s^{-1}, very close to our proposed value. This is an indication that the original selection of the values used for f and k_d as well as the experimental data are correct.

The thermophysical properties as well as all the other kinetic rate constants used in this work were adopted from the work of Hutchinson et al.[41] However, it was found to be convenient to introduce the transfer to monomer kinetic rate constant as an adjustable parameter because different values were reported in literature.[41,43]

4. RESULTS AND DISCUSSION

According to the aforementioned methodology, the kinetic rate constants k_{tc}, k_{td}, k_p, and k_d at low monomer conversions have been defined. The glass effect was assumed negligible as the polymerization takes place at temperatures above the glass transition temperature of the reaction mixture. This leaves only four parameters, i.e., D_{p00}, k_{fM}, D_{I0}/C, and A, to be estimated. For the estimation of these parameters we used the following methodology. All four were assumed to be adjustable in the case of neat PBMA. Best-fit values thus estimated were $D_{p00} = 5.89 \times 10^{14}$ L mol^{-1} s^{-1}, $k_{fM} = 0.2$ L mol^{-1} s^{-1}, $D_{I0}/C = 9.8 \times 10^6$, and $A = 33$. The value estimated for k_{fm} here was much larger than literature values (i.e., 0.0076 in ref 41 and 0.033 in ref 43). The reason could be that this parameter cannot be directly measured independently and is usually estimated from fitting to experimental data. Therefore, k_{fM} was assumed to be constant in all nanocomposites and only three, i.e., D_{p00}, D_{I0}/C, and A were allowed to vary. Using standard nonlinear regression analysis methods, the best-fit values estimated are tabulated in Table 3. It was found that parameter A increases with the amount of the nano-MMT while the parameter D_{I0}/C decreases. Moreover the D_{p00} adjustable parameter remains almost constant. The discrepancy in the A and D_{p00} values observed in the case of 1% nano-MMT could be attributed to possible experimental errors. Using these parameters, the simulation model results on the variation of conversion with time are compared to the experimental data from ref 8 in Figure 2. A very good fit of the experimental data was observed in all different compositions. As can be seen, besides the initial slightly lower reaction rate observed with the addition of the nanoclay, the conversion values in the autoacceleration region decrease as the amount of filler increases.

Table 3. Best-Fit Values of D_{I0}/C, D_{p00}, and A Estimated Using the Simulation Model and the Experimental Data, Assuming $k_{fm} = 0.2$ L mol^{-1} s^{-1} As Obtained from Fitting the Neat PBMA Polymerization Kinetics

	PBMA	PBMA + 1% Cl15A	PBMA + 3% Cl15A	PBMA + 5% Cl15A
D_{I0}/C ($\times 10^{-6}$)	9.8	1.63	1.16	0.82
A ($\times 10^{-2}$)	0.33	0.563	0.487	0.76
D_{p00} ($\times 10^{-14}$)	5.89	4.56	5.57	5.62

dx.doi.org/10.1021/ie501360j | Ind. Eng. Chem. Res. 2014, 53, 11303−11311

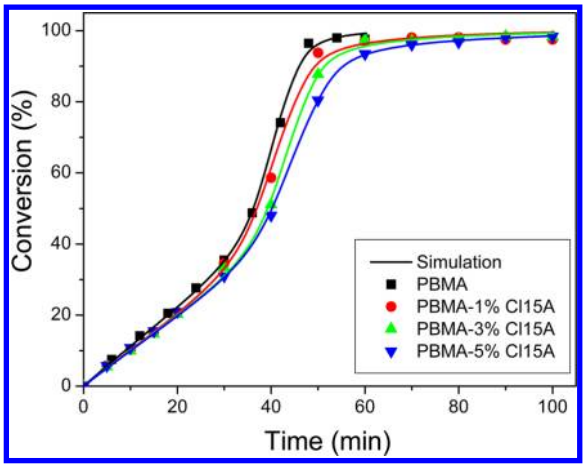

Figure 2. Comparison of the simulation model results to the experimental data for neat PBMA and nanocomposites with different relative amounts of nanoclay (Cloisite 15A). Polymerization at 80 °C with $[I]_0$ = 0.03 M experimental data from ref 8.

To understand the physical phenomena taking place during the reaction, the variation of the termination rate constant as predicted from the simulation model is plotted as a function of monomer conversion for the neat PBMA in Figure 3. From this

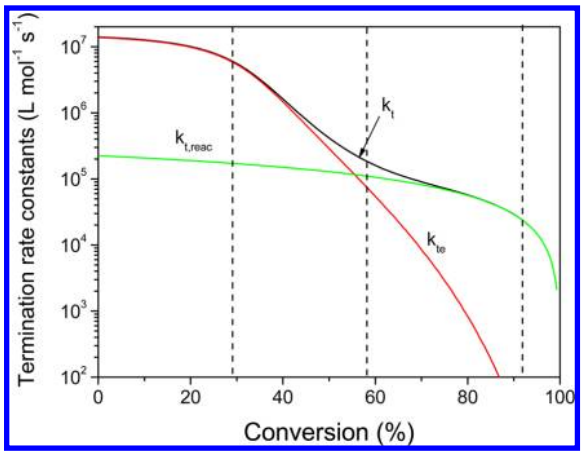

Figure 3. Variation of the overall termination rate constant and its two contributions from the center-of-mass diffusion (k_{te}) and the reaction diffusion ($k_{t,reac}$) with conversion obtained from simulation data of the bulk polymerization of neat PBMA.

figure, four distinctive regimes are clear. In the first, occurring at low monomer conversions (less than 30%), the termination rate constant slightly decreases with conversion and chemical reaction is the dominant mode of termination. At conversion levels higher than 30%, the center-of-mass diffusion of the macromolecular chains is hindered and the k_{te} term is decreased, leading to decreased overall k_t values. At almost 65% conversion, the k_{te} term has been decreased by 3 orders of magnitude and the reaction−diffusion term now starts to play the dominant role. This means that at these conversion levels whole chains cannot move in space but they can implicitly move through the addition of monomer molecules. After that point, k_t equals $k_{t,reac}$ and as a result is proportional to the propagation reaction. At high conversion levels (>90%), most of the monomer has been consumed; thus, M in eq 25 decreases significantly, leading to a decrease in $k_{t,reac}$ and a secondary decrease of the overall k_t.

The variation of the overall termination rate constant with conversion for all different nanocomposites examined appears in Figure 4. From the results of this figure it seems that k_t starts

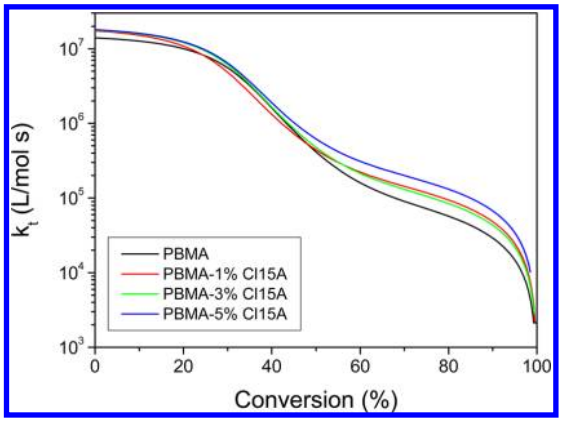

Figure 4. Variation of the overall termination rate constant with conversion for all different nanocomposites examined.

to decrease earlier when nano-MMT is added to the system compared to the neat polymer. Also, the values of the overall termination rate constant in the plateau region (i.e., in the conversion interval where the reaction−diffusion term is the dominant one) are higher as the amount of the nanofiller increase. The conclusions that can be drawn from these curves are that the presence of the clay platelets hinders the center-of-mass diffusion of the macroradicals; therefore, k_{te} starts to decrease earlier. However, the frequency of adding monomer molecules to the live radical chain and thus its implicit movement in space is increased with the amount of nano-MMT added. This is the physical explanation for the increase in the estimated values of the parameter A. The increased k_t at the higher amount of the nanoclay leads to lower local radical concentrations and as a result lower reaction rates and monomer conversion values. Concerning the effect of the addition of the nanoMMT on the initiation reaction, the picture is clear in Figure 5. It is shown that f starts to decrease at relatively lower conversion values as the nanofiller amount increases. This could be attributed to the retardation in diffusion of primary radicals caused by the nanofiller or to possible deactivation reactions of the primary radicals due to the nanofiller. This means that again the presence of the clay

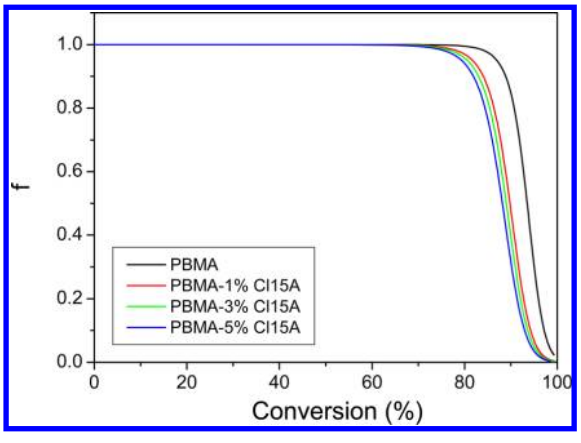

Figure 5. Variation of the initiator efficiency with conversion for all different nanocomposites examined.

dx.doi.org/10.1021/ie501360j | Ind. Eng. Chem. Res. 2014, 53, 11303−11311

platelets poses additional barriers in the movement of small primary radicals; therefore, they cannot easily find a monomer molecule to react, resulting in decreasing f values. The direct consequence of this phenomenon is the lower conversion values measured at very high conversions as the amount of nanoclay increases.

The evolution of the neat PBMA number and weight-average molecular weights with monomer conversion appears in Figures 6 and 7, respectively. As expected, both averages slightly

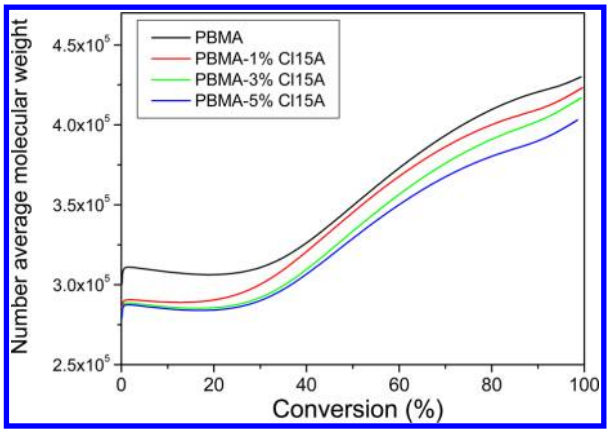

Figure 6. Variation of the polymer number-average molecular weight with conversion for all different nanocomposites examined.

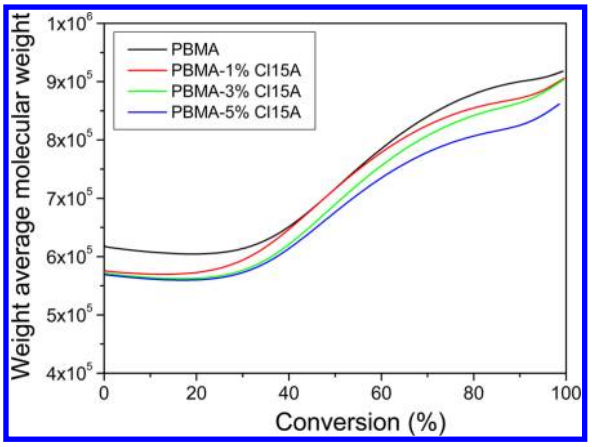

Figure 7. Variation of the polymer weight-average molecular weight with conversion for all different nanocomposites examined.

decrease initially with monomer conversion following classical polymerization kinetics. Afterward, the effect of diffusion-controlled phenomena on the termination rate constant and the increase in the macroradical local concentration leads to the production of macromolecular populations with increased and different chain lengths. This results in the increased polymer average molecular weight and the polydispersity of the MWD. This increase tends to level off at high monomer conversions where f also decreases.

Moreover, the effect of the nanofiller on the variation of the polymer number and weight-average molecular weights with conversion for all different nanocomposites examined is shown in Figures 6 and 7, respectively. The higher termination rate constant predicted at the higher amount of nanoclay added always leads to lower M_n of the nanocomposites compared to neat PBMA. Higher termination rate means that the radicals terminate before they grow enough. Hence, the polymer formed has lower molecular weight. However, concerning the polydispersity of the polymer MWD, it was found that the increased amount of nanoclay did not have any significant influence on the final estimated values ranging between 2.13 and 2.16.

Finally, the variation of the polymer MWD for all different nanocomposites examined is shown in Figure 8 and compared

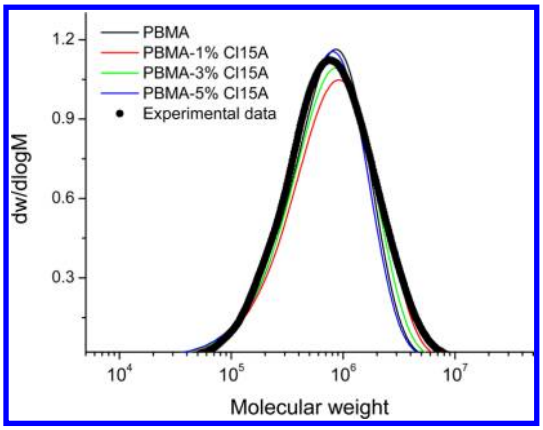

Figure 8. Polymer molecular weight distribution for all different nanocomposites examined and comparison to experimental data.

to experimental data. Typical unimodal distributions were obtained because of relatively low polydispersity and further enhanced by an increased transfer to monomer or depropagation kinetic rate constants. Comparison with experimental data is satisfactory.

5. CONCLUSIONS

The effect of the amount of organo-modified nanoclay on the polymerization kinetics of butyl methacrylate was investigated using a simulation model. The model was based on the elementary reactions taking place and a final set of differential equations describing the variation of the species mass balances with reaction time. Diffusion-controlled phenomena on termination propagation and the initiation reaction were considered through theoretical models with a minimum number of adjustable parameters. Kinetic rate constants at low monomer conversions were taken from the literature, and a critical discussion on their values followed. Simulation model results describe experimental data on the variation of conversion with time at different relative amounts of the nanoclay added to the mixture very well. From the values of the adjustable parameters, very interesting features on the effect of adding the nanoclay on the physical phenomena taking place during the reaction were revealed. Future work should be focused on studying the effect of nanoadditives on other polymerizations, such as the methyl methacrylate (MMA) in situ free-radical polymerization.

AUTHOR INFORMATION

Corresponding Author

*Tel.: +30 2310 997822. Fax: +30 2310 997769. E-mail: axilias@chem.auth.gr.

Notes

The authors declare no competing financial interest.

■ ACKNOWLEDGMENTS

The authors acknowledge the support provided by the Deanship of Scientific Research (DSR) at King Fahd University of Petroleum & Minerals (KFUPM), Dhahran, Saudi Arabia, for funding this work through Project IN101022. The support from the Chemistry Department, Aristotle University of Thessaloniki, Greece, is sincerely appreciated.

■ NOMENCLATURE

A = residual termination adjustable parameter
A_{nc} = entropic barrier model adjustable parameter
D_n; D_n = , "dead" polymer having n monomer units ; its concentration
b = free-volume theory adjustable parameter
D = polydispersity
D_I = primary radicals self-diffusion coefficient
D_{I0} = free-volume theory pro-exponential parameter for primary radicals
D_M = monomer self-diffusion coefficient in the presence of nanoadditive
D_{M0} = monomer self-diffusion coefficient in the absence of nanoadditive
D_{M00} = free-volume theory pro-exponential parameter for monomer self-diffusion
$\bar{D}_p$ = self-diffusion coefficient of macroradicals in the presence of nanoadditive
$\bar{D}_{p0}$ = self-diffusion coefficient of macroradicals in the absence of nanoadditive
D_{p00} = free-volume theory pro-exponential parameter for macroradicals self-diffusion
C/D_I = cage effect parameter
f = initiator efficiency
I; I = initiator; its concentration
k_d = initiator decomposition kinetic rate constant
k_{eff} = overall effective rate constant
k_{t0} = intrinsic termination rate constant defined at zero conversion
k_{fm} = chain transfer to monomer kinetic rate constant
k_p = propagation rate kinetic rate constant
k_t = overall termination kinetic rate constant
k_{tc} = termination by combination kinetic rate constant
k_{td} = termination by disproportionation kinetic rate constant
k_{te} = diffusion-controlled termination kinetic rate constant
$k_{t,reac}$ = reaction−diffusion-controlled kinetic rate constant
M; M = monomer; its concentration
$\bar{M}$ = radicals number-average degree of polymerization
N_A = Avogadro number
P_0 = total concentration of linear "live" radicals
P_n; P_n = "live" polymer having n monomer units; its concentration
PR$^\bullet$; $PR^\bullet$ = primary radical from the fragmentation of the initiator; its concentration
r_t = effective termination reaction radius
R = universal gas constant
t = time
T = temperature
T_g = Glass transition temperature
V = reactor volume
V_f = free-volume fraction
X = fractional monomer conversion
$\bar{X}_n$ = polymer number-average degree of polymerization
$\bar{X}_w$ = polymer weight-average degree of polymerization

Greek Symbols

α = entropic barrier model adjustable parameter
$\delta(n)$ = Kronecker delta
ε = volume contraction factor
λ_n = n moment of "live" radicals chain length distribution
μ_n = n moment of "dead" polymer chain length distribution
ρ_m = monomer density
ρ_p = polymer density
φ_c = volume fraction of nanoadditive

Subscripts

I = initiator
m = monomer
n = number of monomer units in the polymer chain
0 = initial conditions
p = polymer

■ REFERENCES

(1) Giannelis, E. P.; Krishnamoorti, R. K.; Manias, E. Polymer-silicate nanocomposites: Model systems for confined polymers and polymer brushes. *Adv. Polym. Sci.* **1998**, *138*, 107−148.
(2) Pavlidou, S.; Papaspyrides, C. D. A review on polymer−layered silicate nanocomposites. *Prog. Polym. Sci.* **2008**, *33*, 1119−1198.
(3) Zeng, C.; Lee, L. J. Poly(methyl methacrylate) and polystyrene/clay nanocomposites prepared by in situ polymerization. *Macromolecules* **2001**, *34*, 4098−4103.
(4) Li, Y.; Zhao, B.; Xie, S.; Zhang, S. Synthesis and properties of poly(methyl methacrylate)/montmorillonite nanocomposites. *Polym. Int.* **2003**, *52*, 892−898.
(5) Ingram, S.; Dennis, H.; Hunter, I.; Liggat, J. J.; McAdam, C.; Pethrick, R. A.; Schaschke, C.; Thomson, D. Influence of clay type on exfoliation, cure and physical properties of in situ polymerized poly(methyl methacrylate) nanocomposites. *Polym. Int.* **2008**, *57*, 1118−1127.
(6) Nikolaidis, A. K.; Achilias, D. S.; Karayannidis, G. P. Effect of the type of organic modifier on the polymerization kinetics and the properties of poly(methyl methacrylate)/organomodified montmorillonite nanocomposites. *Eur. Polym. J.* **2012**, *48*, 240−251.
(7) Achilias, D. S.; Nikolaidis, A. K.; Karayannidis, G. P. PMMA/organomodified montmorillonite nanocomposites prepared by in situ bulk polymerization: Study of the reaction kinetics. *J. Therm. Anal. Calorim.* **2010**, *102* (2), 451−460.
(8) Achilias, D. S.; Siafaka, P.; Nikolaidis, A. K. Polymerization kinetics and thermal properties of poly(alkyl methacrylate)/organomodified montmorillonite nanocomposites. *Polym. Int.* **2012**, *61*, 1510−1518.
(9) Siddiqui, M. N.; Redhwi, H. H.; Gkinis, K.; Achilias, D. S. Synthesis and characterization of novel nanocomposite materials based on poly(styrene-co-butyl methacrylate) copolymers and organomodified clay. *Eur. Polym. J.* **2013**, *49*, 353−365.
(10) Siddiqui, M. N.; Redhwi, H. H.; Charitopoulou, D.; Achilias, D. S. Effect of organomodified clay on the reaction kinetics, properties and thermal degradation of nanocomposites based on poly(styrene-co-ethyl methacrylate). *Polym. Int.* **2014**, *63*, 766−777.
(11) Moad, G.; Solomon, D. H. *The Chemistry of Radical Polymerization*, 2nd ed.; Elsevier: Amsterdam, The Netherlands, 2006.
(12) Achilias, D.; Kiparissides, C. Modeling of diffusion-controlled free-radical polymerization reactions. *J. Appl. Polym. Sci.* **1988**, *35*, 1303−1323.
(13) Achilias, D. S. A review of modeling of diffusion controlled polymerization reactions. *Macromol. Theory Simul.* **2007**, *16*, 319−347.
(14) Verros, G. D.; Latsos, T.; Achilias, D. S. Development of a unified framework for calculating molecular weight distribution in diffusion-controlled free-radical bulk homo-polymerization. *Polymer* **2005**, *46*, 539−552.
(15) Verros, G.. D.; Achilias, D. S. Modeling gel effect in branched polymer systems: Free-radical solution homopolymerization of vinyl acetate. *J. Appl. Polym. Sci.* **2009**, *111*, 2171−2185.

(16) Achilias, D. S.; Verros, G. V. Modeling of diffusion-controlled reactions in free-radical solution and bulk polymerization: Model validation by DSC experiments. *J. Appl. Polym. Sci.* **2010**, *116*, 1842−56.
(17) Begum, F.; Zhao, H.; Simon, S. L. Modeling methyl methacrylate free radical polymerization: Reaction in hydrophylic nanopores. *Polymer* **2012**, *53*, 3238−3244.
(18) Begum, F.; Zhao, H.; Simon, S. L. Modeling methyl methacrylate free radical polymerization: Reaction in hydrophobic nanopores. *Polymer* **2012**, *53*, 4372−4378.
(19) Zhao, H.; Simon, S. L. Methyl methacrylate polymerization in nanoporous confinement. *Polymer* **2011**, *52*, 4093−4098.
(20) Bamford, C. H.; Barb, W. G..; Jenkins, A. D.; Onyon, D. F. *Kinetics of Vinyl Polymerization by Radical Mechanisms*; Butterworths: London, 1958.
(21) Hamielec, A. E.; Hodgins, J. W.; Tebbens, K. Polymer reactors and molecular weight distribution: Part II. Free radical polymerization in a batch reactor. *AIChE J.* **1967**, *13*, 1087−1091.
(22) Konstadinidis, K.; Achilias, D. S.; Kiparissides, C. Development of a unified mathematical framework for modelling molecular and structural changes in free-radical homopolymerization reactions. *Polymer* **1992**, *33*, 5019−5031.
(23) Achilias, D. S.; Sideridou, I. D. Kinetics of the benzoyl peroxide/amine initiated free radical polymerization of dental dimethacrylate monomers: Experimental studies and mathematical modeling for TEGDMA and Bis-EMA. *Macromolecules* **2004**, *37*, 4254−4265.
(24) Gam, S.; Meth, J. S.; Zane, S. G.; Chi, C.; Wood, B. A.; Seitz, M. E.; Winey, K. I.; Clarke, N.; Composto, R. J. Macromolecular diffusion in a crowded polymer nanocomposite. *Macromolecules* **2011**, *44*, 3494−3501.
(25) Vrentas, J. S.; Duda, J. L. Diffusion in polymer-solvent systems I. Re-examination of the free-volume theory. *J. Polym. Sci. Polym. Phys. Ed.* **1977**, *15*, 403−416.
(26) Vrentas, J. S.; Duda, J. L. Diffusion in polymer-solvent systems II. A predictive theory for the dependence of diffusion coefficients on temperature, concentration and molecular weight. *J. Polym. Sci. Polym. Phys. Ed.* **1977**, *15*, 417−439.
(27) Ju, S. T.; Duda, J. L.; Vrentas, J. S. Influence of temperature on diffusion of solvents in polymers above the glass transition. *Ind. Eng. Chem., Prod. Res. Dev.* **1981**, *20*, 330−335.
(28) Ju, S. T.; Liu, H. T.; Duda, J. L.; Vrentas, J. S. Solvent Diffusion in amorphous polymers. *J. Appl. Polym. Sci.* **1981**, *26*, 3735−3744.
(29) Muthukumar, M.; Baumgartner, A. Effect of entropic barriers on polymer dynamics. *Macromolecules* **1989**, *22*, 1937−1941.
(30) Muthukumar, M.; Baumgartner, A. Diffusion of a polymer-chain in random-media. *Macromolecules* **1989**, *22*, 1941−1946.
(31) Muthukumar, M. Entropic barrier model for polymer diffusion in concentrated polymer solutions and random media. *J. Non-Cryst. Solids* **1991**, *131*, 654−666.
(32) Delgadillo-Velázquez, O.; Vivaldo-Lima, E.; Quintero-Ortega, I. A.; Zhu, S. Effects of diffusion-controlled reactions on atom-transfer radical polymerization. *AIChE J.* **2002**, *48*, 2597−2608.
(33) Sun, X. Y.; Luo, Y. W.; Wang, R.; Li, B. G.; Zhu, S. P. Semibatch RAFT polymerization for producing ST/BA copolymers with controlled gradient composition profiles. *AIChE J.* **2008**, *54*, 1073−1087.
(34) D'hooge, D. R.; Reyniers, M.-F.; Marin, G.. B. Methodology for kinetic modeling of Atom Transfer Radical Polymerization. *Macromol. Reac. Eng.* **2009**, *3*, 185−209.
(35) Zhou, Y.-N.; Li, J.-J.; Luo, Z.-H. Synthesis of gradient copolymers with simultaneously tailor-made chain composition distribution and glass transition temperature by semibatch ATRP: From modeling to application. *J. Polym. Sci., Part A: Polym. Chem.* **2012**, *50*, 3052−3066.
(36) D'hooge, D. R.; Reyniers, M.-F.; Marin, G.. B. The crucial role of diffusional limitations in controlled radical polymerization. *Macromol. React. Eng.* **2013**, *7*, 362−379.
(37) Davis, T. P.; O'Driscoll, K. F.; Piton, M. C.; Winnik, M. A. Copolymerization propagation kinetics of styrene with alkyl methacrylates. *Macromolecules* **1990**, *23*, 2113−2119.
(38) Kamachi, M.; Kajiwara, A. ESR estimation of propagation rate constants of radical polymerization of butyl methacrylate. *Macromol. Chem. Phys.* **2000**, *201*, 2160−64.
(39) Buback, M.; Junkers, T. Termination kinetics of *tert*-butyl methacrylate and *n*-butyl methacrylate free-radical bulk homopolymerizations. *Macromol. Chem. Phys.* **2006**, *207*, 1640−1650.
(40) Barth, J.; Buback, M.; Hesse, P.; Sergeeva, T. Chain-length-dependent termination in *n*-butyl methacrylate and *tert*-butyl methacrylate bulk homopolymerizations studied via SP-PLP-ESR. *Macromolecules* **2009**, *42*, 481−488.
(41) Wang, W.; Hutchinson, R. A.; Grady, M. C. Study of butyl methacrylate depropagation behavior using batch experiments in combination with modeling. *Ind. Eng. Chem. Res.* **2009**, *48*, 4810−4816.
(42) Wang, W.; Hutchinson, R. A. A comprehensive kinetic model for high-temperature free radical production of styrene/methacrylate/acrylate resins. *AIChE J.* **2011**, *57*, 227−238.
(43) Li, D.; Hutchinson, R. A. High temperature semibatch free radical copolymerization of styrene and butyl methacrylate. *Macromol. Symp.* **2006**, *243*, 24−34.
(44) Davis, T. P.; Matyjaszewski, K. *Handbook of Radical polymerization*. Wiley-Interscience: Hoboken, NJ, 2002.
(45) Odian, G. *Principles of Polymerization*, 4th Ed. Wiley-Interscience: Hoboken, NJ, 2004.
(46) Chanda, M. *Introduction to Polymer Science and Chemistry*. CRC Taylor & Francis: Boca Raton, FL, 2006.
(47) www.Aldrich.com (accessed February 26, 2014).
(48) Stickler, M.; Dumont, E. Free radical polymerization of methyl methacrylate at very high conversions. 2. Study of the kinetics of initiation by benzoyl peroxide. *Makromol. Chem.* **1986**, *187*, 2663−2673.
(49) Li, D.; Li, N.; Hutchinson, R. A. High-temperature free radical copolymerization of styrene and butyl methacrylate with depropagation and penultimate kinetic effects. *Macromolecules* **2006**, *39*, 4366−4373.